Cross section measurements of deuteron induced nuclear reactions on natural tungsten up to 34 MeV

C. Duchemin, Arnaud Guertin, Ferid Haddad, Nathalie Michel, Vincent Métivier

Cross section measurements of deuteron induced nuclear reactions on natural tungsten up to 34 MeV

C. Duchemin[a], A. Guertin[a], F. Haddad[a,b], N. Michel[a,b], V. Métivier[a]

[a] *SUBATECH, Ecole des Mines de Nantes, Université de Nantes, CNRS/IN2P3, Nantes, France*

[b] *GIP Arronax, 1 rue Aronnax, 44817 Saint-Herblain, France*

Abstract

HIGHLIGHTS

- Deuteron induced reactions on natural tungsten up to 34 MeV.
- Experimental values determined using the stacked-foil technique.
- Comparison with the TALYS code version 1.6.
- Thick target yield of ^{186g}Re, ^{183,182g,184m,184g,181}Re and ^{187}W.

ABSTRACT

^{186g}Re is a β-/γ emitter of great interest for nuclear medicine. It has shown successful results on bone metastases palliation and has similar chemical properties as ^{99m}Tc, the most commonly used imaging agent. ^{186g}Re is routinely produced using rhenium target in nuclear reactor. Higher specific activity could be obtain using accelerators. In this paper, production cross section values are presented for the ^{nat}W(d,x)^{186g}Re reaction up to 34 MeV, using the stacked-foils method and gamma spectrometry. From this data set, the thick target production yield of ^{186g}Re is determined and compared with the validated values of the IAEA and also with the proton route. The production cross sections of the ^{nat}W(d,x)^{183,182g,184m,184g,181}Re and ^{nat}W(d,x)^{187}W reactions have also been determined. A good agreement is found with the literature. Our data are compared with the version 1.6 (December 2013) of the TALYS code which shows discrepancies both on the shape and on the amplitude for these deuteron induced reactions.

Email address: Charlotte.Duchemin@subatech.in2p3.fr (C. Duchemin)

Keywords: tungsten target, deuteron beam, stacked-foil technique, excitation function, TALYS 1.6

1. Introduction

In the field of medical radioisotope production, the knowledge of the activation cross section allows to quantify and control the production of a radionuclide. ^{186g}Re ($T_{1/2}$ = 3.7 days), is a β- emitter which has been used in clinical trials for palliation of painful bone metastases resulting from prostate and breast cancer (Palmedo et al., 2001). This radionuclide is currently produced with nuclear reactor using ^{185}Re enriched target or aluminum perrhenate target (Ishfaq et al., 1999; Ehrhardt et al., 1997; Knapp Jr et al., 1997, Ehrhardt et al., 1996). These production routes lead to a low specific activity. To obtain high specific activity product, ^{186g}Re could be advantageously produced on a tungsten target with cyclotrons able to accelerate deuterons or protons (Guertin et al., 2013). This paper reports activation cross section values and thick target production yields for the ^{nat}W(d,x)^{186g,184m,184g,183,182g,181}Re and ^{nat}W(d,x)^{187}W reactions up to 34 MeV. These data are compared with the literature and the TALYS code calculations (Koning and Rochman, 2012). This large set of data is of interest for the International Fusion Materials Irradiation Facility project (IFMIF) in the estimation of the deuteron-activation of structural materials (Gobin et al., 2009) and could help to constrain theoritical codes on cross section predictions.

2. Materials and methods

2.1. Experimental set-up

Cross section measurements are made using the stacked-foils method (Duchemin et al., 2014; Guertin et al., 2013). A set of thin foils is irradiated containing 10 μm thick tungsten targets, 10 μm thick titanium monitor foils to have informations on the beam flux and thick aluminium degrader foils (between 100 and 500 μm) to change the incident beam energy, which impinged the tungsten foils.

The ARRONAX cyclotron delivers a deuteron beam with an energy within $\pm$ 0.25 MeV (Haddad et al., 2008). All along the stack, depending on the number of foils, the energy uncertainty calculated using the SRIM

software (Ziegler et al., 2010) increases up to ± 0.7 MeV due to the energy straggling. Several stacks were irradiated with a different incident energy in order to minimize this energy dispersion and cover the full energy range from 34 MeV down to the reaction thresholds. This way, we were also able to overlap data points and be sure that our experiments are under control. Typical irradiations were carried out with a beam intensities between 80 and 200 nA for 30 minutes. Irradiation conditions are reported in Table 1.

The stacks were irradiated with an external deuteron beam, delivered by the ARRONAX cyclotron. A 75 μm thick kapton foil closes the line and makes a barrier between the air in the vault and the vacuum in the beam line. The stacks were located about 7 cm downstream in air. The energy through each thin foil was determined in the middle of the thickness of the foil using the SRIM software (Ziegler et al., 2010). Energy loss in the kapton foil and air were taken into account.

All foils were purchased from Goodfellow® with high purity ($> 99.6\%$). The natural isotopic compositions of the foils are reported in Table 2. Each thin foil has been weighed before irradiation using an accurate scale ($\pm\ 10^{-5}$g) and scanned to precisely determine their area. From these values and assuming that the thickness is homogeneous over the whole surface, the thickness is deduced. A Faraday cup was placed after the stack to collect charges and control the intensity during the irradiation. Titanium monitor foils have been placed behind each target foil, to record the particle flux all along the stack through the ^{nat}Ti(d,x)^{48}V reaction as recommended by the IAEA (Tárkányi et al., 2001).

The activity measurements in each target and monitor foils were performed using a high purity germanium detector from Canberra (France) with low-background lead and copper shielding. All foils were counted twice: starting the day after the irradiation (for few hours) and after 2 or 3 weeks (for more than 48 hours). Gamma spectra were recorded in a suitable geometry calibrated in energy and efficiency with standard ^{57,60}Co and ^{152}Eu gamma sources from LEA-CERCA (France). Samples were placed at a distance of 19 cm from the detector in order to reduce the dead time and pile-up. The dead time during the counting was always below 10%.

2.2. Data processing

The activity values of the produced radioisotopes were derived from the γ spectra and the nuclear decay data given in Table 3, using the Fitzpeak spectroscopy software (FitzPeaks Gamma Analysis and Calibration Software

version 3.66). Knowing the precise thickness of the foil and the activity value of the produced isotope, its cross section is calculated using the well-known activation formula (Duchemin et al., 2014; Guertin et al., 2013). The chemical purity of the sample was taking into account: 99.95% for W and 99.6% for Ti.

As each target is followed by a titanium monitor foil, which receive the same deuteron flux, the cross section is deduced with a relative calculation using the recommended ^{nat}Ti(d,x)^{48}V cross section. The ^{48}V activity was extracted using the γ lines at 944.13, 983.525 and 1312.106 keV (Ekström, and Firestone, 2004). The uncertainty on the production cross section is calculated as a quadratic form (Duchemin et al., 2014; Guertin et al., 2013). Main errors come from the measured activity (from 5 to 40% in W target and up to 2% for ^{48}V), the thickness of the foils (around 1%) and the uncertainty on the ^{48}V recommended cross section (around 12%). The contribution of the irradiation time is not significant and has been neglected.

2.3. Comparison with the TALYS 1.6 code

TALYS is a nuclear reaction program to simulate reaction induced by light particles on nuclei heavier than carbon. It incorporates many theoretical models to predict physical parameters including theoretical cross section values as a function of the incident particle energy (from 1 keV to 1 GeV). In this work, all the experimental cross section values are compared with the last version (1.6) of the TALYS code (december, 2013), with default parameters (Koning and Rochman, 2012).

3. Results

Our activation cross section results for the ^{nat}W(d,x)^{186g}Re reaction are presented in this section, as well as those of the other radionuclides produced in our target, and detectable by our device, which are of interest in the specific activity determination. No fission products or tantalum radioisotopes have been detected, as there are under the detection limit of our device. These data are plotted as full circles in Figures 1 to 7 and compared with the published experimental values (EXFOR database, National Nuclear Data Center), and with the results obtained with the TALYS code. The numerical values are reported in Table 5. The thick target yields of the ^{nat}W(d,x)^{186g,183,182g,184m,184g,181}Re and ^{nat}W(d,x)^{187}W reactions are presented at the end of this paper.

3.1. Production of ^{186g}Re

^{186g}Re has a half-life of 3.7183 days and decays at 92.53% by β- to ^{186}Os (stable) and at 7.47% by EC to ^{186}W (stable). Its gamma line, $E_\gamma = 137.157$ keV ($I_\gamma = 9.42$ (6) %), coming from the β- decay, is used to measure the activity (see Table 3). We supposed that the metastable state ^{186m}Re contribution is negligeable due to its very long half-life (2.10^5 years) compared with our experiment duration. ^{186g}Re can only come from the ^{186}W (with an isotopic abundance of 28.6%), via the reaction ^{186}W(d,2n)^{186g}Re. It is then possible to extract, from our data, the production of ^{186g}Re considering an enriched target. Our data set is presented in Figure 1 with others results previously published, the values recommended by the IAEA (Tárkányi et al., 2013) and the version 1.6 of the TALYS code. Our results are very close to Zhenlan et al., 1981, in the range 7 to 12 MeV. Tárkányi et al., 2003, and Hishioka et al, 2006, have contributed with higher energy beams. Our results are in good agreement, especially with Tárkányi et al., 2003. The results of Hishioka et al., 2006, are higher than ours. The TALYS code doesn't give satisfactory results, especially on the amplitude.

3.2. Production of ^{181}Re

^{181}Re has a half life of 19.9 hours and decays by electron capture (EC) to ^{181}W ($T_{1/2} = 121$ days). Its gamma line at 365.570 keV ($I_\gamma = 56$ (6) %) was used to determined the activity. Two others gamma lines with lower branching ratio (reported in Table 3), identified in the spectrum, lead to comparable activities. ^{181}Re experimental cross section is plotted in Figure 2 with a linear scale (a) and a logarithmic scale (b). Logarithmic scale allows to show the contribution of the ^{180}W(d,n) reaction between 0 to 12 MeV. This tungsten isotope has a very low isotopic abundance (0.1%), which explains the small contribution to the cross section. The linear scale lets appreciate the maximum of the cross section at 26 MeV with 350 mbarn. Looking at the contributing reactions in Table 4, this maximum is mainly due to the reactions on the ^{182}W and ^{183}W isotopes. Our values can be compared with Tárkányi et al., 2003 and Hishioka et al., 2002. They are in agreement taking into account the uncertainty bars. These errors are mainly due to the 11% of uncertainty on the gamma line used to determine the activity. The TALYS 1.6 code give results close to the experimental values.

3.3. Production of ^{182g}Re

^{182g}Re, with a half life of 64 hours, emits several gamma lines between 130 and 1427 keV (see Table 3), which are not common with its metastable state. ^{182m}Re doesn't feed the ground state. The activity extracted from each of this gamma lines were in total agreement giving us confidence in our values. Our ^{nat}W(d,xn)^{182g}Re production cross section values are plotted in Figure 3 and compared with the work of Tárkányi et al., 2003. ^{182g}Re can be produced on four of the five isotopes constituting the natural tungsten target. These reaction channels, with threshold values reported in Table 4, can be easily identified on the experimental activation cross section trend. Compared to Tárkányi et al, 2003, our results are in good agreement but with values slightly higher between 20 and 28 MeV. The TALYS code pretty well reproduced the trend and the different reaction channels but overestimate the cross section up to 30 % in some cases.

3.4. Production of ^{183}Re

The decay of ^{183}Re is accompanied by three main gamma radiations presented in Table 3. It can be produced on the same tungsten isotopes as ^{182g}Re, previously presented. Our results are plotted in Figure 4 with three other data sets. These data show that the maximum cross section is around 22 MeV but with a different magnitude depending on the series. Our new values are similar to those of Tárkányi et al., 2003 and are in agreement with Nakao et al., 2006 only between 23 and 33 MeV. Significant differences with Hishioka et al., 2002 are observed on the whole energy range. The TALYS code gives a good trend up to 25 MeV even if the magnitude is underestimated. However, from this point, the cross section seems to be shifted towards lower energies.

3.5. Production of ^{184m}Re and ^{184g}Re

^{184m}Re, with a half life of 169 days, decays by IT (74.5%) to the ground state ^{184g}Re and by EC (25.5%) to ^{184}W. Three γ lines summarized in Table 3 permit to extract the ^{184m}Re activity. ^{184m}Re production cross section is plotted in Figure 5 with the results of Zhenlan et al., 1981. The comparaison can be made only up to 15 MeV, because no experimental data have been already published above this energy. Our results are always below the data of Zhenlan et al., 1981. From 15 MeV, our new experimental data set has the same shape as TALYS.

^{184g}Re, with a half life of 38 days, decays by EC (100%) to ^{184}W. We have previously seen that ^{184g}Re is fed by ^{184m}Re. As both states have some γ lines in common but also different ones, we were able to extract the activity of ^{184g}Re without the direct production contribution of ^{184m}Re. The activity values retrieved from the three γ lines summarized in Table 3 were in total agreement. The contribution coming from the decay of ^{184m}Re strongly depends of the measuring time. In our experiments, the gamma spectra are recorded the day after the irradiation for few hours and again several days after the irradiation for more than 24 hours in order to get lower uncertainties on the long half-life radionuclides. In the case of ^{184g}Re, we used the second counting to extract the cross section values. The contribution of ^{184m}Re is up to 2.9 % of the total ^{184g}Re activity and has been substracted. The independant excitation function of ^{184g}Re is plotted in Figure 6 with Tárkányi et al., 2003, results. In this latter publication, the authors assume a maximum of 0.2% of ^{184m}Re contribution. Both experiments are in good agreement. Additional data points have been measured for the lower energy part in our experiment. The TALYS code gives a shifted trend compared to the experimental results, as observed for ^{183}Re and ^{184m}Re, and the amplitude is not reproduced.

3.6. Production of ^{187}W

^{187}W is the only tungsten radioisotope we were able to measure. The others tungsten isotopes may be produced but their gamma lines have too low branching ratio (less than 0.09%) to be detected by our experimental tools.

^{187}W with a half life of 23.72 hours decreases at 100% by β- to ^{187}Re (stable). It can be detected with different γ lines (see Table 3) with branching ratio higher than 4%, which result in a small uncertainty on the cross section determination. Our results are plotted in Figure 7 with previous data. Up to 10.5 MeV, our results perfectly follow the Andelin et al., 1964, values. From 11 MeV, our data set is totally in agreement with Tárkányi et al., 2003. In comparison with the other data, the maximum of the curve is different depending on the series. Indeed, around 12 MeV, our values are 13% lower than Andelin et al., 1964, between 14 to 40% lower than Hishioka et al, 2002 and 15% higher than Zhenlan et al., 1981. The TALYS code underestimates by 50 % the amplitude.

3.7. Thick target yield (TTY)

Using the cross section values obtained in this work, we have calculated for each radionuclide produced. Their thick target yield (TTY) in Bq/μA.h as a function of the projectile energy, using the relation (1).

$$TTY = \Phi.\chi.\frac{N_a.\rho}{A}(1 - e^{-\lambda.t}) \int_{Emin}^{Emax} \frac{\sigma(E)}{\frac{dE}{dx}} dE \quad (1)$$

Where χ is the target enrichment and $\frac{dE}{dx}$ is the specific energy loss of the projectile in the target material (MeV.cm^{-1}). In a thick target, the incident particle energy decrease with the penetration depth. E_{max} corresponds to the incident projectile energy when it enters into the target whereas E_{min} corresponds to its energy when it leaves the target. It can also be called production yield or integral yield. The TTY of the different radionuclides produced in the ^{nat}W are plotted in Figure 8 and reported in Table 6 for the maximum energy 33.4 MeV.

3.7.1. ^{186g}Re production on a natural tungsten target

The IAEA estimates that the integral yield of ^{nat}W(d,x)^{186g}Re (Trknyi et al., 2013) is 7.5 MBq/μA.h at 33 MeV against 8.5 MBq/μA.h with our experimental values (Figure 9). This difference can be accounted to the IAEA recommended cross section fit (plotted in Figure 1), which draw a peak slightly thinner and lower than our points. Other authors have calculated the ^{186g}Re thick target yield since the IAEA recommendation. Hermanne et al., in 2009, obtained values in agreement with the recommended thick target yield of the IAEA whereas Bonardi et al., in 2010, published data up to 30 % higher. With protons, the recommended integral yield published by the IAEA (Trknyi et al., 2013) is 2.7 MBq/μA.h at 33 MeV (Figure 9). The deuteron production route is clearly the best choice for the production of this medical radioisotope.

3.7.2. ^{186g}Re production on an enriched tungsten target

For medical applications, the production of contaminants has to be avoided. An easy way to produce ^{186g}Re without contaminants is to use a 100% enriched ^{186}W target irradiated with deuteron beams. When using this tungsten isotope as target, only the ^{186g}Re and ^{184m,g}Re could be produced. With a deuteron energy just below the ^{186}W(d,4n)^{184m,g}Re reaction threshold, 17.6 MeV (Table 4), the ^{186g}Re specific activity will be the greatest possible with a

TTY of 16.8 MBq/μA.h to be compared with the IAEA recommended value of 15.4 MBq/μA.h with deuterons and 4.6 MBq/μA.h with a proton beam at the same energy.

4. Conclusion

In this paper are presented experimental cross section values for the ^{nat}W(d,x)^{186g,184m,184g,183,182g,181}Re and ^{nat}W(d,x)^{187}W reactions, up to 34 MeV. Comparison with previous data sets show that our results are in good agreement with Tarkanyi et al., 2003. This study presents for the first time the experimental ^{nat}W(d,x)^{184m}Re production cross section above 15 MeV. The thick target yields of all the produced radionuclides are shown. For the medical radioisotope ^{186g}Re, the yields show a production three times higher using deuteron as compared to proton as projectile. For these deuteron induced reactions, a comparison with the TALYS code (version 1.6) have been made with default parameters. It shows discrepancies both on the amplitude and on the shape. Additional data using deuterons on other targets are needed to better constrain the nuclear models.

5. Acknowledgments

The ARRONAX cyclotron is a project promoted by the Regional Council of Pays de la Loire financed by local authorities, the French government and the European Union. This work has been, in part, supported by a grant from the French National Agency for Research called "Investissements d'Avenir", Equipex Arronax-Plus n^o ANR-11-EQPX-0004 and Labex n^o ANR-11-LABX-0018-01.

6. References

Blessing, G., Bräutigam, W., Böge, H.G., Gad, N., Scholten, B., and Qaim, S.M., 1995. Internal irradiation system for excitation function measurement via the stacked-foil technique, Appl. Radiat. Isot. 955, 46-9.

Bonardi, M.L., Groppi, F., Persico, E., Manenti, S., Abbas, K., Holzwart, U., Simonelli, F., Alfassi, Z. B., 2011. Excitation functions and yields for cyclotron production of radiorhenium via natW(p, xn)181-186gRe nuclear reactions and tests on the production of 186gRe using enriched 186W. Radiochim. Acta 99, 1-11.

Bonardi, M.L., Groppi, F., Manenti, S., Persico, E., Gini, L., 2010. Production study of high specific activity NCA Re-186g by proton and deuteron cyclotron irradiation. Appl. Radiat. Isot. 68, 1595-1601.

Duchemin, C., Guertin, A., Haddad, F., Michel, N., Métivier, V., 2014. 232Th(d,4n)230Pa Cross Section Measurements at ARRONAX facility for the production of 230U, Nuclear Medicine and Biology (in press, corrected proof - doi:10.1016: j.nucmedbio.2013.12.011).

Ehrhardt, G.J., Blumer, M.E., Su, F.M., Vanderheyden, J.L., Fritzberg, A.R., 1996. Experience with Aluminium Perrhenate targets for Reactor Production of High Specific Activity Re-186. Appl. Radiat. Isot. 48-1, 1-4.

Ehrhardt, G.J., Ketring, A.R., Ayers, L.M., 1997. Reactor-produced Radionuclides at the University of Missouri research Reactor. Appl. Radiat. Isot. 49-4, 295-297.

Ekström, L.F., and Firestone, R.B., 2004. Information extracted from the Table of Radioactive Isotopes, version 2.1.

FitzPeaks Gamma Analysis and Calibration Software version 3.66, produced by JF Computing Services (UK), based on methods presented in Nucl.Instrum. and Methods (1981) 190, 89-99, describing the program SAMPO80 of the Helsinki University of Technology, Finland.

Gobin, R. et al. General design of the IFMIF deuteron injector: source and beam line, Proc. of ICIS09, Gatlinburg Tennessee, USA.

Guertin, A., Duchemin, C., Haddad, F., Michel, N., Métivier, V., 2013. Measurements of 186Re production cross section induced by deuterons on natW target at ARRONAX facility, Nuclear Medicine and Biology (In press, corrected proof - DOI:10.1016/j.nucmedbio.2013.11.003).

Haddad, F., Ferrer, L., Guertin, A., Carlier, T., Michel, N., Barbet, J., Chatal, J.F., 2008. Arronax a high-energy and high-intensity cyclotron for nuclear medicine, Eur. J. Nucl. Med. Mol. Imaging 35, 1377-1387.

Hermanne, A., Daraban, L., Tárkányi, F., Takács, S., Ditrói, F., Ignatyuk, A., Adam Rebeles, R., Bada, M., 2009. Excitations functions for some W, Ta and Hf radionuclides obtained by deuteron irradiation of 181Ta up to 40 MeV. Nuclear Instruments and Methods in Physics Research B 267, 3293-3301.

Ishfaq, M.M., Mushtaq, A., Jawaid, M., 1999. Experience on the neutron activation of natural/enriched Re, Sm, and Ho nuclides in a reactor for the production of radiotherapeutic radionuclides. Biol. Trace Elem. Res. 71-2, 519-526.

Ishioka, N.S., Watanabe, S., Osa, A., Koizumi, M., Matsuoka, H., Sekine,

T., 2002. Excitation Functions of Rhenium Isotopes on the natW(d,xn) Reactions and Production of No-carrier-addied 186Re. J. Nucl. Sci. Technol supplement 2, 1334-1337.

Knapp Jr, F.F(RUSS), Mirzadeh, S., Beets, A.L., O'Doherty, M., Blower, P.J., Verdera, E.S., Gaudiano, J.S., Kropp, J., Guhlke, J., Palmedo, H., Biersack, H.J., 1997. Reactor-produced radioisotopes from ORNL for Bone Pain Pallation. Appl. Radiat. Isot. 49-4, 309-315.

Koning, A.J., Rochman, D., 2012. Modern nuclear data evaluation with the TALYS code system, Nucl. Data Sheets 113, 2841.

Nakao, M., Hori, J., Ochiai, K., Kubota, N., Sato, S., Yamauchi, M., Ishioka, N.S., Nishitani, T., 2006. Measurements of deuteron-induced activation cross-sections for IFMIF accelerator structural materials. Nucl. Instrum. Methods Phys. Res., Sect. A 562, 785.

National Nuclear Data Center, information extracted from the NuDat2 database, http://www.nndc.bnl.gov/nudat2/.

Palmedo, H., Rockstroh, J.K., Bangard, M., Schliefer, K., Risse, J., Menzel, C., Biersack, H.J., 2001. Painful Multifocal Arthritis: Therapy with Rhenium 186 Hydroxyethylidenedi-phosphonate (186Re HEDP) after Failed Treatment with Medication-Initial Results of a Prospective Study. Radiology 221, 256-260.

Tárkányi, F., Takács, S., Gul, K., Hermanne, A., Mustafa, M.G., Nortier, M., Oblozinsky, P., Qaim, S.M., Scholten, B., Shubin, Yu.N., Youxiang, Z., 2001. Beam monitor reactions, in Charged Particle Cross Section Database for Medical Radioisotope Production: Diagnostic Radioisotopes and Monitor Reactions; IAEA-TECDOC-1211, pages 49-152, IAEA, Vienna. Database available on https://www-nds.iaea.org/medportal/, update may 2013.

Tárkányi, F., Takács, S., S., Szelecsenyi, F., Ditroi, F., Hermanne, A., Sonck, M., 2003. Excitation functions of deuteron induced nuclear reactions on natural tungsten up to 50 MeV. Nucl. Instrum. Methods Phys. Res., Sect. B 211, 319-330.

Zhenlan, T., Fuying, Z., Huiyuan, Q., Gongqing, W., 1981. Excitation functions for 182-186W(d,2n)182-186Re and 186W(d,p)187W reactions. Chin. J. Nucl. Phys. 3, 242.

Ziegler, J.F., Ziegler, M.D., Biersack, J.P., 2010. SRIM The stopping and range of ions in matter, Nucl. Instrum. Methods Phys. Res., Sect. B 268, 1818-1823.

Table 1: Irradiation conditions

Beam energy (MeV)	<Intensity> (nA)	Energy points (MeV)				
34.00 (25)	206	33.36 (30)	32.13 (35)	27.91 (49)	23.11 (59)	20.93 (63)
30.75 (25)	141	30.06 (29)	26.35 (41)	24.39 (46)	19.85 (58)	18.43 (64)
16.90 (25)	113	14.67 (38)	13.32 (43)	11.85 (50)	10.42 (56)	8.85 (66)
30.75 (25)	105	22.37 (55)				
22.59 (25)	101	16.96 (31)				
16.90 (25)	82	15.52 (33)	12.87 (44)	9.74 (57)		

Table 2: Isotopic composition of natural Ti and W foils from Goodfellow®

^{46}Ti	^{47}Ti	^{48}Ti	^{49}Ti	^{50}Ti
8.0 %	7.5 %	73.7 %	5.5 %	5.3 %
^{180}W	^{182}W	^{183}W	^{184}W	^{186}W
0.1 %	26.3 %	14.3 %	30.7 %	28.6 %

Table 3: Produced radioisotope parameters (National Nuclear Data Center; Ekström and Firestone, 2004)

Radioisotope	$T_{1/2}$	E_γ(keV)	I_γ(%)
^{181}Re	19.9 (7) h	365.570	56 (6)
		953.420	3.6 (9)
		639.30	6.4 (13)
^{182g}Re	64.0 (5) h	130.80	7.5 (5)
		169.151	11.3 (8)
		191.380	6.7 (5)
		256.450	9.5 (8)
		276.311	8.7 (5)
		286.554	7.0 (5)
		339.060	5.6 (4)
		351.070	10.3 (8)
		1076.30	10.5 (3)
		1427.00	9.79 (18)
^{183}Re	70.0 (11) d	162.322	23.30 (40)
		208.8057	2.95 (5)
		291.724	3.05 (16)
^{184g}Re	38.0 (5) d	792.07	37.5 (6)
		894.757	15.6 (3)
		903.28	37.9 (6)
^{184m}Re	169 (8) d	104.729	13.40 (40)
		318.012	5.75 (8)
		920.932	8.14 (12)
^{186g}Re	3.7183 (11) d	137.157	9.42 (6)
^{187}W	23.72 (6) h	479.531	21.8 (4)
		551.532	5.08 (11)
		618.361	6.28 (14)
		685.774	27.3 (6)
		772.890	4.12 (8)

Table 4: Contributing reactions and threshold (National Nuclear Data Center)

Radioisotope	Contributing reaction(s)	$E_{threshold}$ (MeV)
^{181}Re	^{180}W(d,n)	0.00
^{182g}Re	^{182}W(d,2n)	5.87
	^{183}W(d,3n)	12.13
	^{184}W(d,4n)	19.62
	^{186}W(d,6n)	32.71
^{183}Re	^{182}W(d,n)	0.00
	^{183}W(d,2n)	3.60
	^{184}W(d,3n)	11.09
	^{186}W(d,5n)	24.18
^{184g}Re	^{183}W(d,n)	0.00
	^{184}W(d,2n)	4.54
	^{186}W(d,4n)	17.62
^{184m}Re	^{183}W(d,n)	0.00
	^{184}W(d,2n)	4.54
	^{186}W(d,4n)	17.62
^{186}Re	^{186}W(d,2n)	3.63
^{187}W	^{186}W(d,p)	0.00

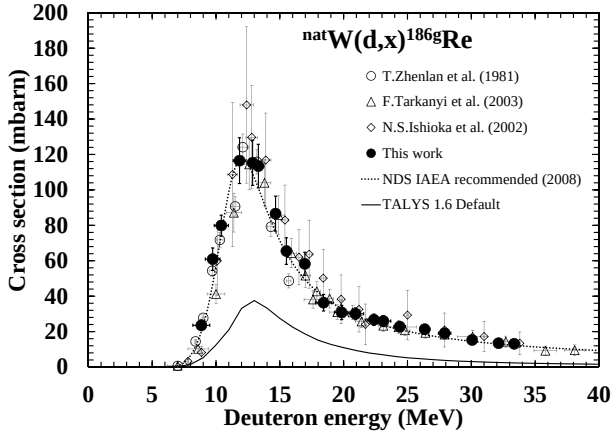

Figure 1: ^{nat}W(d,x)^{186g}Re production cross section

Table 5: Experimental cross section values (mbarn) for ^{nat}W(d,x)^{186g,183,182g,184m,184g,181}Re and ^{187}W reactions

Energy (MeV)	σ ^{186g}Re (mb)	σ ^{183}Re (mb)	σ ^{182g}Re (mb)	σ ^{184m}Re (mb)
8.85 ± 0.66	23.56 ± 2.96	19.71 ± 3.11	1.71 ± 0.24	
9.74 ± 0.57	60.90 ± 6.33	43.17 ± 4.61	7.91 ± 0.85	2.50 ± 0.47
10.42 ± 0.56	79.89 ± 5.87	53.77 ± 4.67	11.49 ± 0.94	
11.85 ± 0.50	116.51 ± 12.92	79.68 ± 9.31	25.83 ± 3.04	8.41 ± 4.31
12.87 ± 0.44	115.29 ± 12.75	118.12 ± 13.42	43.52 ± 4.94	16.50 ± 2.13
13.32 ± 0.43	113.42 ± 12.32	130.35 ± 14.75	47.44 ± 6.22	14.20 ± 4.34
14.67 ± 0.38	86.59 ± 9.89	211.68 ± 25.16	74.99 ± 8.87	16.03 ± 8.31
15.52 ± 0.33	65.47 ± 7.50	261.83 ± 30.73	87.73 ± 10.32	22.35 ± 2.88
16.96 ± 0.31	58.24 ± 6.54	295.79 ± 34.33	98.64 ± 11.72	21.06 ± 4.34
18.43 ± 0.64	36.30 ± 4.68	376.98 ± 48.81	115.92 ± 15.32	9.80 ± 2.03
19.85 ± 0.58	30.78 ± 4.02	414.37 ± 53.82	116.87 ± 15.28	8.67 ± 2.23
20.93 ± 0.63	30.04 ± 3.33	415.95 ± 46.85	117.55 ± 13.28	12.05 ± 2.60
22.37 ± 0.55	26.70 ± 3.19	431.84 ± 51.13	136.85 ± 16.02	
23.11 ± 0.59	25.95 ± 2.98	424.43 ± 50.06	131.51 ± 15.51	37.00 ± 5.30
24.39 ± 0.46	22.81 ± 2.94	354.27 ± 43.15	168.30 ± 20.55	61.47 ± 8.80
26.35 ± 0.41	21.34 ± 2.67	261.75 ± 32.16	212.54 ± 25.31	96.90 ± 13.24
27.91 ± 0.49	19.07 ± 2.25	215.60 ± 25.42	211.65 ± 25.26	108.31 ± 13.52
30.06 ± 0.29	15.29 ± 1.88	188.56 ± 23.19	239.99 ± 28.99	112.82 ± 14.35
32.13 ± 0.35	13.46 ± 1.67	241.05 ± 28.84	226.45 ± 27.22	96.28 ± 11.73
33.36 ± 0.30	13.13 ± 1.64	269.91 ± 32.11	228.05 ± 27.19	89.87 ± 11.22

Table 5 (continued) : Experimental cross section values (mbarn) for ^{nat}W(d,x)^{186g,183,182g,184m,184g,181}Re and ^{187}W reactions

Energy (MeV)	σ ^{184g}Re (mb)	σ ^{181}Re (mb)	σ ^{187}W (mb)
8.85 ± 0.66	26.97 ± 3.48	0.09 ± 0.04	35.10 ± 4.41
9.74 ± 0.57	69.09 ± 7.33	0.10 ± 0.04	58.60 ± 6.0
10.42 ± 0.56	91.36 ± 6.97	0.13 ± 0.07	63.07 ± 4.73
11.85 ± 0.50	138.45 ± 15.55		67.28 ± 8.11
12.87 ± 0.44	181.02 ± 20.37	0.17 ± 0.07	69.76 ± 7.84
13.32 ± 0.43	178.67 ± 19.66		65.28 ± 7.21
14.67 ± 0.38	164.93 ± 19.04	4.15 ± 1.08	61.17 ± 7.06
15.52 ± 0.33	129.66 ± 15.08	26.66 ± 7.94	56.69 ± 6.64
16.96 ± 0.31	115.80 ± 13.19	45.60 ± 13.58	53.78 ± 6.26
18.43 ± 0.64	60.59 ± 7.71	200.33 ± 50.16	40.30 ± 5.17
19.85 ± 0.58	63.04 ± 8.05	252.12 ± 63.40	37.07 ± 4.79
20.93 ± 0.63	70.82 ± 7.78	259.40 ± 62.80	35.26 ± 3.91
22.37 ± 0.55		328.27 ± 87.77	33.17 ± 3.94
23.11 ± 0.59	138.26 ± 15.94	304.32 ± 74.72	30.07 ± 3.46
24.39 ± 0.46	203.43 ± 24.19	341.61 ± 92.70	27.85 ± 3.60
26.35 ± 0.41	246.10 ± 28.50	350.30 ± 94.91	24.38 ± 3.20
27.91 ± 0.49	260.34 ± 30.37	276.96 ± 93.77	22.01 ± 5.00
30.06 ± 0.29	219.86 ± 25.92	268.76 ± 73.30	16.80 ± 2.12
32.13 ± 0.35	191.94 ± 22.45	220.30 ± 69.32	15.28 ± 2.75
33.36 ± 0.30	170.04 ± 19.84	256.14 ± 72.95	14.85 ± 1.91

Table 6: Thick-target yield (TTY) of the different produced radionuclides at 33.4 MeV

Radionuclide	TTY (MBq/μA.h)
^{181}Re	203.2
^{182g}Re	45.7
^{183}Re	3.1
^{184g}Re	3.5
^{184m}Re	0.3
^{186g}Re	8.5
^{187}W	28.8

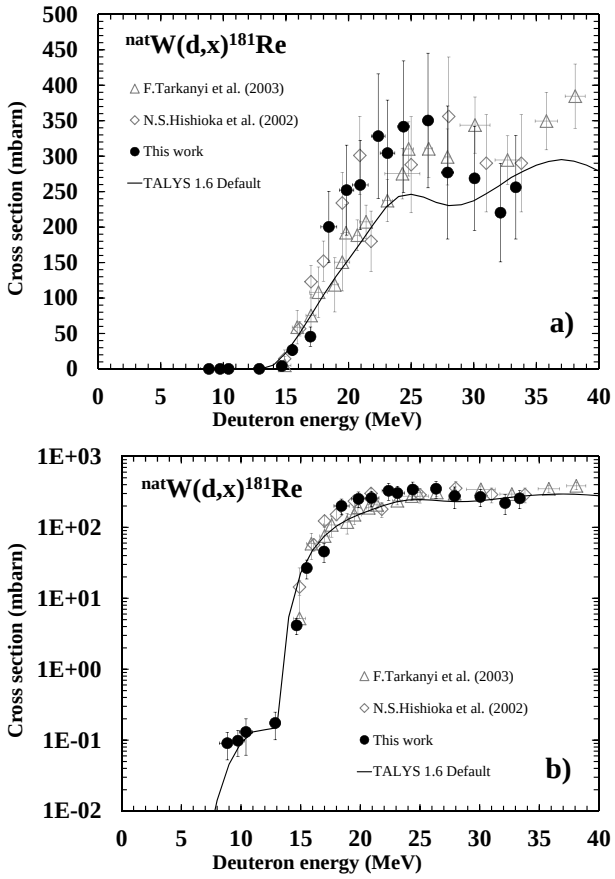

Figure 2: ^{nat}W(d,x)^{181}Re production cross section - linear scale (a), logarithmic scale (b)

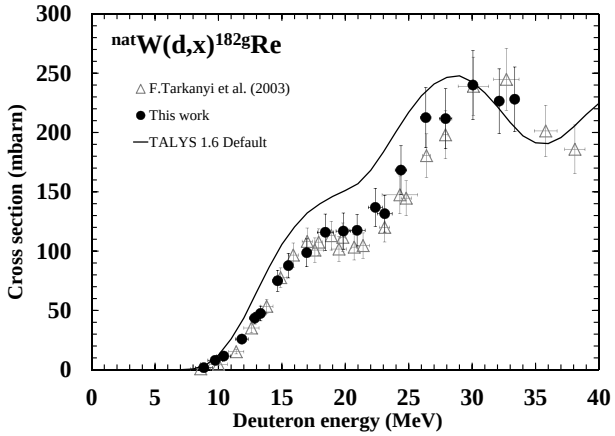

Figure 3: ^{nat}W(d,x)^{182g}Re production cross section

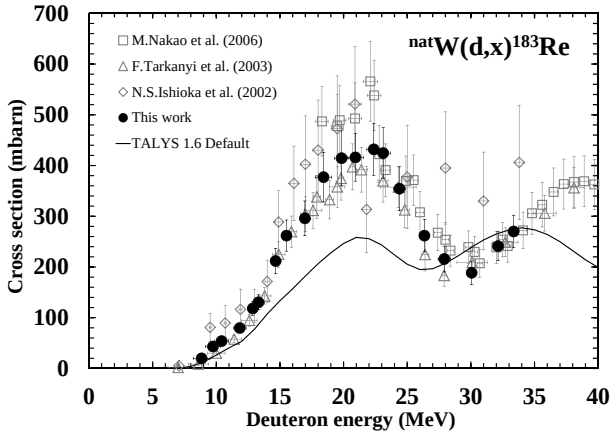

Figure 4: ^{nat}W(d,x)^{183}Re production cross section

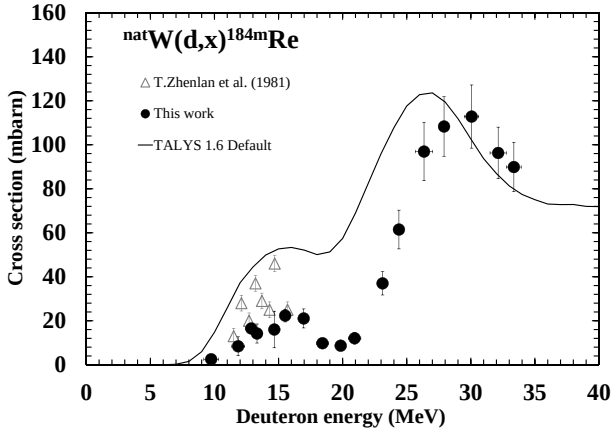

Figure 5: ^{nat}W(d,x)^{184m}Re production cross section

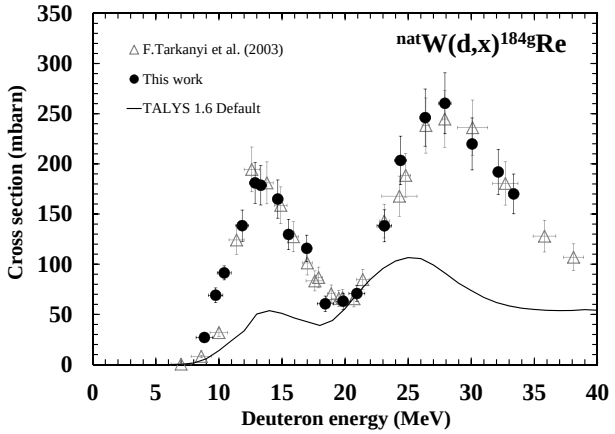

Figure 6: ^{nat}W(d,x)^{184g}Re production cross section

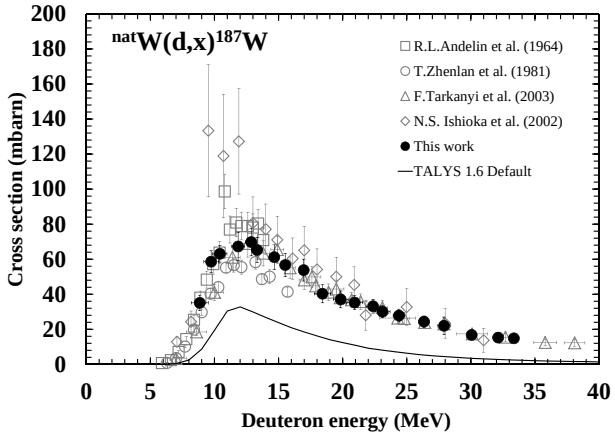

Figure 7: ^{nat}W(d,x)^{187}W production cross section

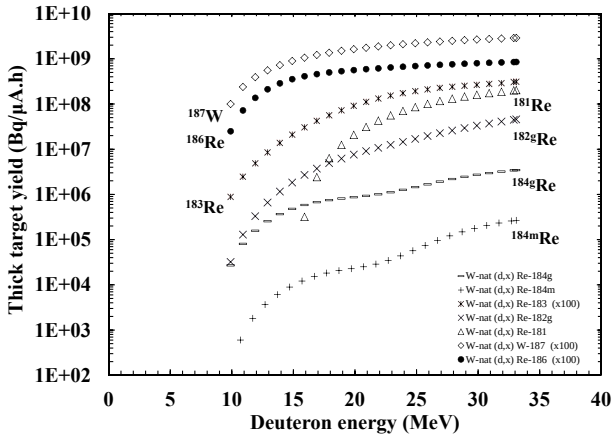

Figure 8: Thick target yield of the produced radionuclides on ^{nat}W in Bq/μA.h

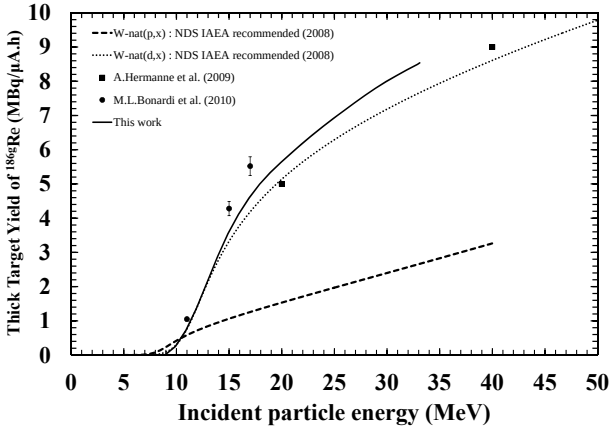

Figure 9: Comparison of the thick target yields of ^{186g}Re in MBq/μA.h